SERPENTINE MINERALS FROM MANITOBA

COLIN J. A. COATS[1]
Department of Geology, University of Manitoba, Winnipeg

ABSTRACT

Serpentinized ultramafic rocks of Aphebian age occur along a northeasterly trending zone of complexly faulted gneissic rocks in the Setting Lake-Moak Lake region of central Manitoba. The predominant serpentine mineral in these rocks is a fibrous variety which can only by satisfactorily indexed on the basis of a 3-layer structure. The derived 3-layer orthorhombic, pseudohexagonal cell has dimensions of $a = 5.346$ Å, $b = 9.205$ Å and $c = 21.93$ Å. Antigorite and lizardite from the area have also been identified by optical, x-ray diffraction and differential thermal analysis methods. Additional occurrences of antigorite from Oxford Lake, Carrot River, Knee Lake and Island Lake in Manitoba and Lancaster Co. in Pennsylvania are described and compared with the Caracas antigorite.

INTRODUCTION

Within the Churchill Province, serpentinized ultramafic rocks of Aphebian age occur along a northeasterly trending narrow zone of complexly faulted gneissic rocks in the Setting Lake-Moak Lake region of central Manitoba. The ultramafic rocks are dunites, peridotites and minor pyroxenites, for the most part entirely converted to serpentinite. They occur in an environment, and possess the form, mineralogy and composition, of typical alpine-type ultramafic rocks. The region in which these rocks occur is presently the focal point for active mining and exploration for nickel ore and is designated the Manitoba nickel belt. A compilation and summary of the geological setting for the ultramafic rocks along the nickel belt has been prepared by Coats (1966) from available published data on the region.

Serpentinite occurrences outside the immediate area of the nickel belt, from which serpentine material has been used in the preparation of this paper, have varied geological environments (Fig. 1). Elongate bodies of serpentinite associated with gabbro at the Oxford Lake and Carrot River occurrences have been described by Barry (1960). At Island Lake, specimens of serpentinite were obtained from an exposed reef and a few small islands approximately 1 mile east of Linklater Island. The sheared and serpentinized peridotite at this locality is apparently a sill or series of sills within highly altered volcanic and sedimentary rocks of the Hayes River Group. There is some question however, whether these ultramafic bodies were intruded along fault

[1]Present address, Falconbridge Nickel Mines Ltd., Box 1530, The Pas, Manitoba.

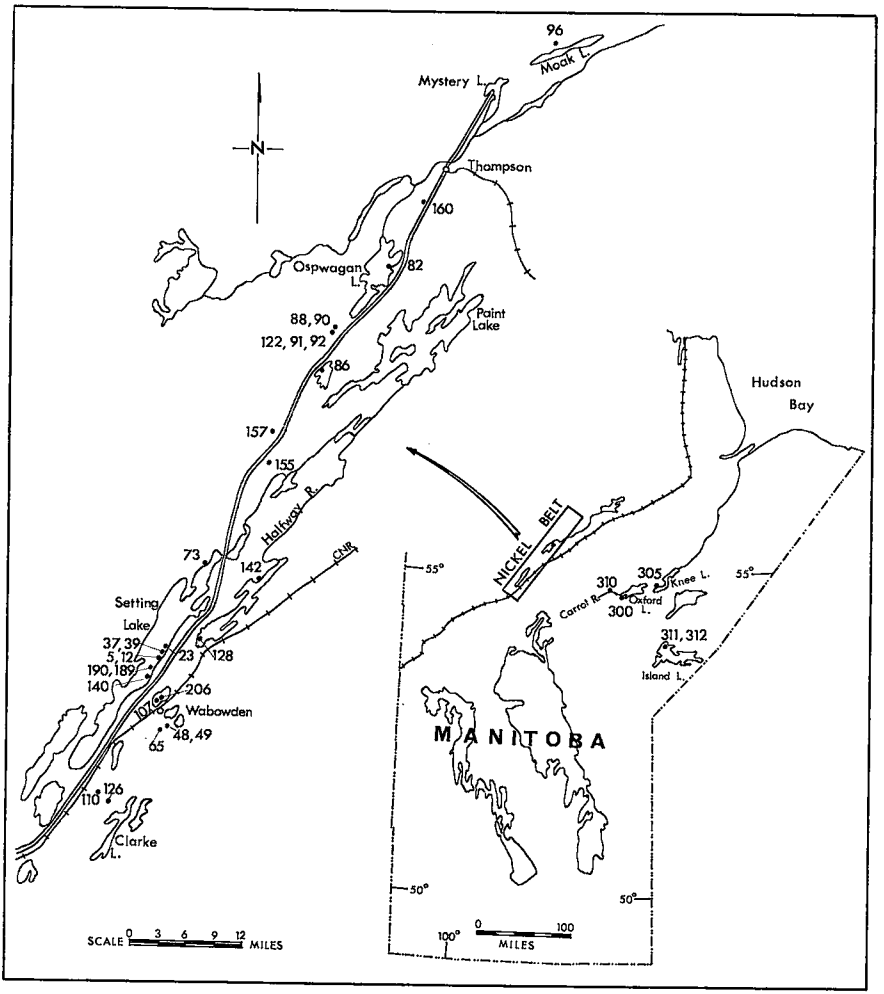

FIG. 1. Map showing location of the serpentine samples.

zones, geologic contacts, or highly schistose zones (Godard 1963). At Knee Lake, an oval-shaped body of partially serpentinized peridotite occurs in dacites and rhyolites of the Hayes River Group (Barry 1959). Gabbroic phases noted in some outcrops of this body indicates differentiation. but the most eastern exposures show the rock to be sheared and almost completely serpentinized.

The location of all specimens from Manitoba serpentinites described in this report is shown on Fig. 1.

Methods of Study

X-ray diffraction data were obtained on powdered serpentine material using a Philips *x*-ray diffractometer. Samples were *x*-rayed in spinning shallow sample holders, using radiation from a copper tube operating at 50kv and 20ma, with a nickel filter. Scan speed was 1° of 2θ per minute and a time constant of 2 seconds. Scale setting for most runs was 4×10^2, a full chart width thus corresponding to 400 counts/second. A scale setting of 1×10^3 was occasionally found useful. Diffraction patterns for all samples were made in the range 10°–75° 2θ.

In the conversion of 2θ to d spacings the Charts for Solution of Bragg's Equation by Parrish & Mack (1963), were used. In these CuK_α is 1.5418 Å.

The apparatus used for differential thermal analysis (DTA) was an R. L. Stone Co. model DTA-13M with controlled atmosphere equipment. Curves for the serpentine minerals were all made over the temperature range 25° C. to 1000° C. at a heating rate of 10° C. per minute. Thermograms were recorded on Leeds and Northrup Speedomax H strip charts with a width of 7 inches. Sensitivity of the thermogram recorder was 150 microvolts for the full chart width. All samples were heated in air with a furnace starting voltage of 44 volts using powdered alumina (−150+200 mesh) in the standard cell.

The curves were calibrated using quartz as a standard and recorded temperature measurements are estimated to be within ±5° C. of their true values.

Petrology and Morphology of the Serpentines

Fibrous serpentines

The predominant serpentine mineral in the ultramafic rocks of the Manitoba nickel belt is a fibrous variety resembling chrysotile. Textural patterns of the serpentines present in massive serpentinite rocks are varied in detail but may be broadly divided into three groups.

a. Mesh serpentine, with more or less regularly disposed phases of alpha serpentine (negative elongation) and gamma serpentine (positive elongation).
b. Close packed cross-fibre veinlets showing pronounced parallelism within the confines of each pseudomorph.
c. Highly irregular system of cross-fibre veinlets and inter-vein serpentine.

Mesh texture serpentine is invariably fine-grained, and composed of a pseudo-rectangular arrangement of cross-fibre veinlets. Considerable

variation is evident in the arrangement of the cross hatching, and in separate specimens the veinlets may outline areas of matrix which are rectangular, equidimensional, lensoid or highly asymmetrical. A sub-rectangular mesh pattern is illustrated in Fig. 2. It is possible to recognize pseudomorph boundaries in many specimens of mesh serpentine, by fine encircling threads of secondary magnetite combined with slight changes in orientation of the mesh. The veinlets themselves are rarely greater than 0.1 mm in width, with fibres arranged normal to the vein margins. Bipartite and tripartite veinlets are the rule, with the two or three sets of parallel fibres abutting near the centre line. The latter is generally marked by a thin film of magnetite dust. Under high magnification, it is common to find dusty magnetite dispersed among the fibres as well. The fibres composing the veinlets have grey to greyish-yellow birefringence, negative elongation and parallel extinction. Their optic orientation identifies them as alpha serpentine (Selfridge 1936).

Matrix material is used here as a general term for the variable constituents occupying the centres of the alpha serpentine mesh. The matrix is generally nearly isotropic and may be amorphous in some cases, but this has yet to be verified. Material of this type has previously been called serpophite (Deer, Howie & Zussman 1962). These authors suggest that

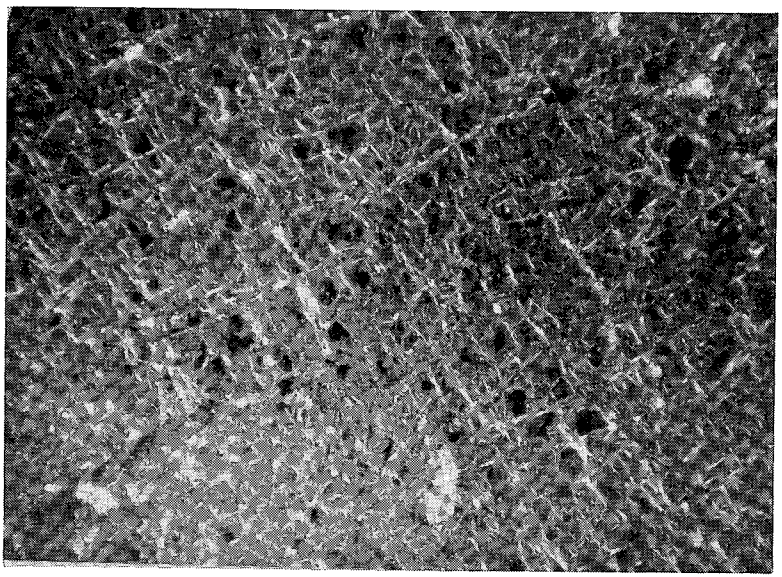

FIG. 2. Sub-rectangular mesh texture serpentine with evenly disseminated anhedral magnetite grains. Margins of fibrous alpha serpentine (white) enclose pale yellowish isotropic material. #12—Setting Lake. (×34).

the isotropic cores of mesh structure could be amorphous material of serpentine, olivine or enstatite composition or alternatively that the distinction between alpha and gamma serpentine and the isotropic components, may be one of different orientations of a single material. Fibrous structure is evident in most mesh centres however, but there is always a distinctly lower birefringence than that shown by the alpha serpentine of the meshes. Mesh centres are colourless to pale shades of yellowish-green and brown. Under high magnification, the fibrous aspect of mesh centres is seen to be due to numerous interwoven fibrolamellar platelets each with individual extinction, or to a continuous smooth surfaced area with a diffuse wavy extinction pattern. Elongation is generally positive and fibrous material of this type has been referred to as gamma serpentine.

Mesh centres are commonly the preferred sites for alteration to take place, leaving the alpha serpentine rims unaltered. Carbonate, carbonate with dusty magnetite inclusions, carbonate with hematite or hematite alone may all occur as fine-grained replacements within the outer rim of the alpha serpentine mesh.

The second general texture of the serpentinites is that of more or less distinct pseudomorphs after olivine, composed of closely packed, parallel, cross-fibre veinlets. A gradation exists between symmetrical mesh textures and parallel vein textures, where one set of veinlets is more highly developed to the exclusion of the other and leaving little matrix material (Fig. 3). Parallelism of veinlets making up one pseudomorph may conform to adjacent pseudomorphs in a specimen, suggesting a preferred orientation of the original olivine before serpentinization. Distinctly different orientations of adjacent pseudomorphs have also been noted. As with the alpha serpentine of mesh texture, the fibres of the close packed veinlets have negative elongation. Vein centres are commonly a thin seam or train of magnetite granules. Variation in birefringence at intervals along the fibres gives the effect of zoning to some veins, and the pattern may be repeated in adjacent veins.

The third division of serpentinite textures is a minor one, and includes specimens with highly irregular cross-fibred veinlets of alpha serpentine showing no particular pattern. Poorly developed mesh textures in this group contain gamma serpentine or finely divided nearly-isotropic material.

Optical orientation of fibrous serpentines

When examined in detail, the mesh texture and parallel vein serpentinites described above show numerous differences of structure and optical orientation. Fig. 4 illustrates a number of mesh textures and vein struc-

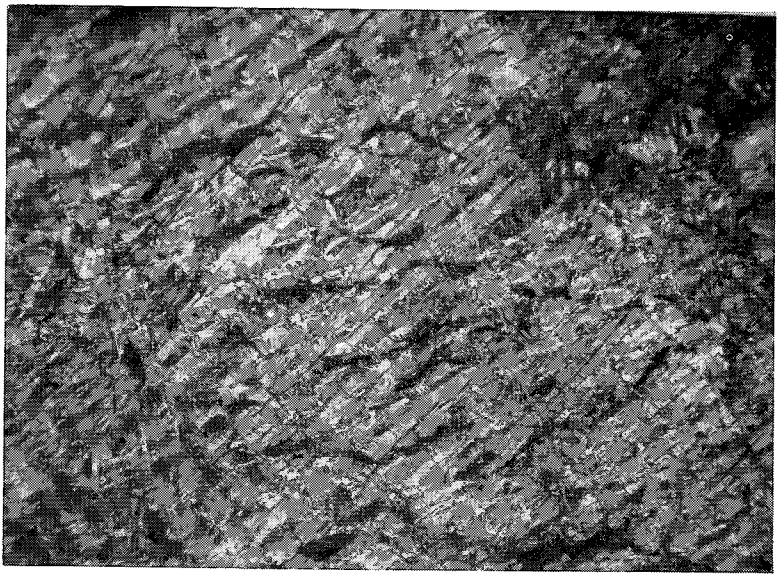

FIG. 3. Closely spaced, sub-parallel veinlets of fibrous serpentine outlining a single pseudomorph. Secondary magnetite has aggregated into stringy lenses. #37—Setting Lake. (×31).

tures of fibrous serpentine selected from samples in these groups. Two fibre types are recognized in the optical studies, namely alpha serpentine, which is length-fast and hence has negative elongation, and gamma serpentine, which is length-slow and considered to have positive elongation. In the mesh textures, alpha serpentine forms the rims and gamma serpentine the cores (Fig. 4D, F, G) or the reverse arrangement may be the case, where gamma serpentine forms the rims and alpha serpentine the cores (Fig. 4I). The optical orientation of the fibres in some veinlets is shown in Fig. 4C, E, and H. In some specimens, narrow, finely fibrous median stems of gamma serpentine with feathery margins of alpha serpentine constitute a veinlet which is separated from adjacent veinlets by trains of magnetite granules (Fig. 4C). The vein system in Fig. 4E consists of a branching series of cross-fibre alpha serpentine veinlets with fibrous, but nearly isotropic serpentine of the same orientation occupying the surrounding areas. The thin median strip of the veinlets has high birefringence and may be clear or contain a row of magnetite grains. Broad marginal bands with sweeping extinction characterize the veinlet in Fig. 4H. The central bipartite zone is alpha serpentine, which is bounded by low birefringent zones and wide marginal zones of fibres, all of gamma serpentine.

The additional structures illustrated in Fig. 4A, B, J and K are

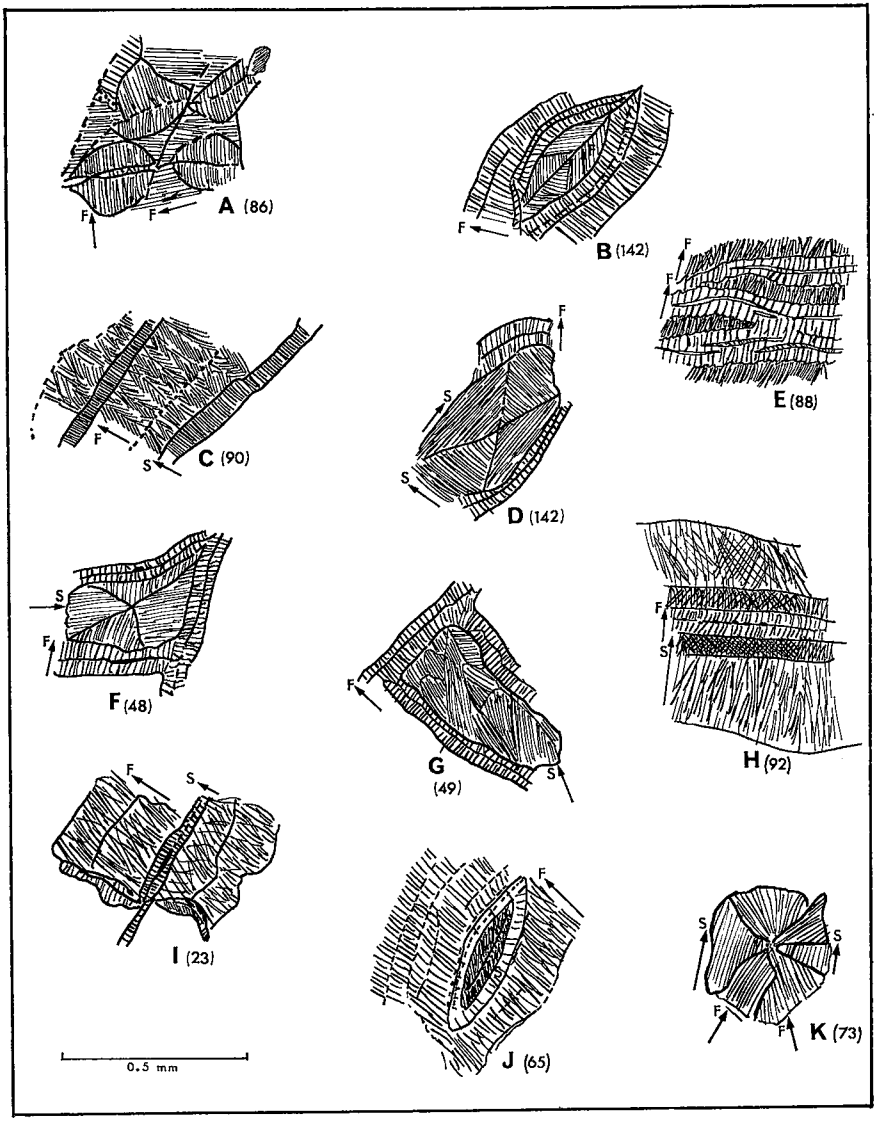

FIG. 4. Textural patterns and optical orientation of some fibrous Manitoba serpentines. F—length-fast, negative elongation, S—length slow, positive elongation.

textural patterns with distinctly different forms from those previously described, but which undoubtedly have a similar origin. Fig. 4A is the diagrammatic representation of the texture in Fig. 5. The mutually interfering fibre systems adjoin at magnetite-filled partings, and all

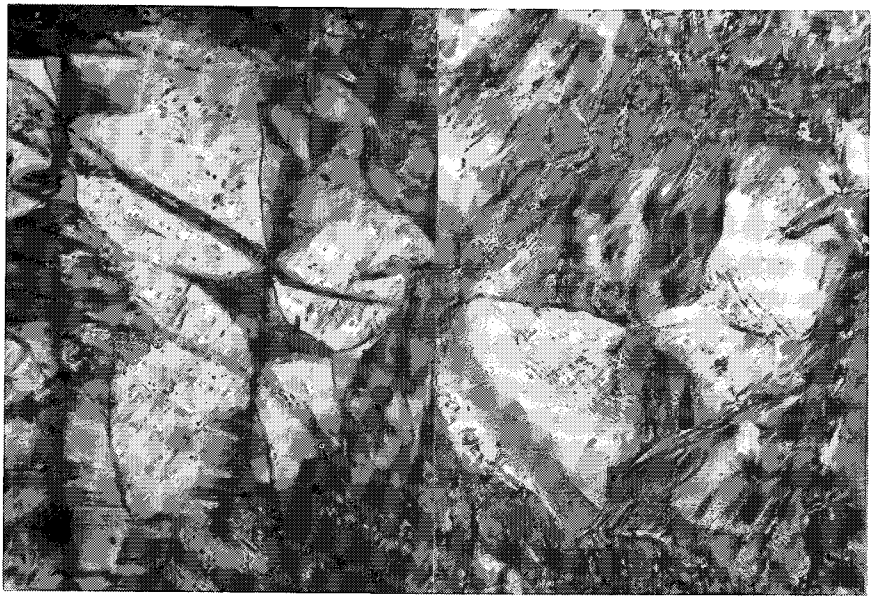

FIG. 5. Leaf-shaped arrangement of the fibres in alpha serpentine. Fine magnetite grains are concentrated in the partings. #86—Joey Lake. (×191).

FIG. 6. Segmented arrangement of fibrous serpentine showing flamboyant extinction. Two of the segments (upper right and lower left) are of gamma serpentine with different attitude to the remaining radial alpha serpentine. #73—North Setting Lake. (×112).

fibres have negative elongation. Textures shown in Figs. 4B and 4J are similar except that the fibrous material of the lensoid areas, enclosed by veinlets of alpha serpentine, has opposite orientation. In Fig. 4B, alpha serpentine with opposing herring-bone textures forms the central area, whereas in Fig. 4J the central area is composed of gamma serpentine. A star-shaped pattern of fibres with flamboyant extinction is illustrated in Fig. 6 and diagrammatically presented in Fig. 4K. The serpentine platelet is segmented into six areas, two of which contain gamma serpentine and the remaining four alpha serpentine. The latter radiate out from a central point, while the fibres of the former lie parallel to one another.

The variable optical orientation of fibrous chrysotile has been discussed by Francis (1956). Chrysotile fibres have a layered structure parallel to (001) and are identical to platy antigorite, except that they are rolled into tubes or hollow cylinders with the fibre axis corresponding to the *a* crystallographic direction, which is parallel to the *Y* optical direction. In measuring the fibre elongation, *Y* is compared with a mean

of X and Z. If the fibre type is optically negative, with X as the acute bisectrix, the velocity of vibrations along Y will be less than the mean and the fibre will have positive elongation. This would explain the optical orientation of gamma serpentine. Similarly, the negative elongation of alpha serpentine can be explained by a change from $2V(-)$ to $2V(+)$. In this case the vibration of Y parallel to the fibre axis would be faster than the mean of X and Z and the fibre would have negative elongation. It can be seen that a change of $2V$ and optic sign can account for the variable birefringence exhibited by many fibrous serpentines. From $2V_z$ acute in alpha serpentine to $2V_x$ acute in gamma serpentine requires a change through $2V = 90°$. The commonly seen, nearly isotropic fibrous material probably has this optical arrangement.

Antigorite

Antigorite serpentinite has been identified from only one locality along the nickel belt. It forms an outcrop about 300 feet wide on a peninsula jutting out from the east shore of Ospwagan Lake (Fig. 1). As indicated on a map by Zurbrigg (1963), the outcrop constitutes part of the east appendage of a highly irregular ultramafic body which underlies the greater part of the lake. In hand specimen the rock is dark green, fine grained and massive.

The antigorite occurs as elongated subrectangular flakes with a maximum length of 1.6 mm. Most exhibit rather ragged and feathery terminations. Poikilitic pseudomorphs after pyroxene and olivine are preserved in well developed textural patterns. These consist of areas, about 6 × 4 mm in size, composed of rounded to oval shaped granules of fine antigorite set in a matrix of antigorite and closely spaced rows of fine magnetic grains (Fig. 7). Within some of the granules, which are pseudomorphic after olivine, the antigorite flakes have an interwoven radial arrangement. Much of the remainder of the rock is composed of a tightly compacted matte of elongate, fibrolamellar flakes of antigorite. Some small areas show a preferred alignment of flakes associated with partings of fine magnetic grains (Fig. 8). These probably represent original pyroxenes and so should correctly be termed bastites. Most bastites occurring in mesh serpentine have a chrysotile or lizardite structure (Whittaker & Zussman 1956), but in this case, we have textures indicative of a pyroxene and olivine-rich ultramafic rock which is now entirely composed of antigorite.

Optically the antigorite has a fibrolamellar, platy form with crystals being generally elongated parallel to the trace of the (001) cleavage. Most have ragged, feathery terminations. Extinction is straight, $(-)$ $2V = 45°$ (approx.), and elongation is positive. Identification has been

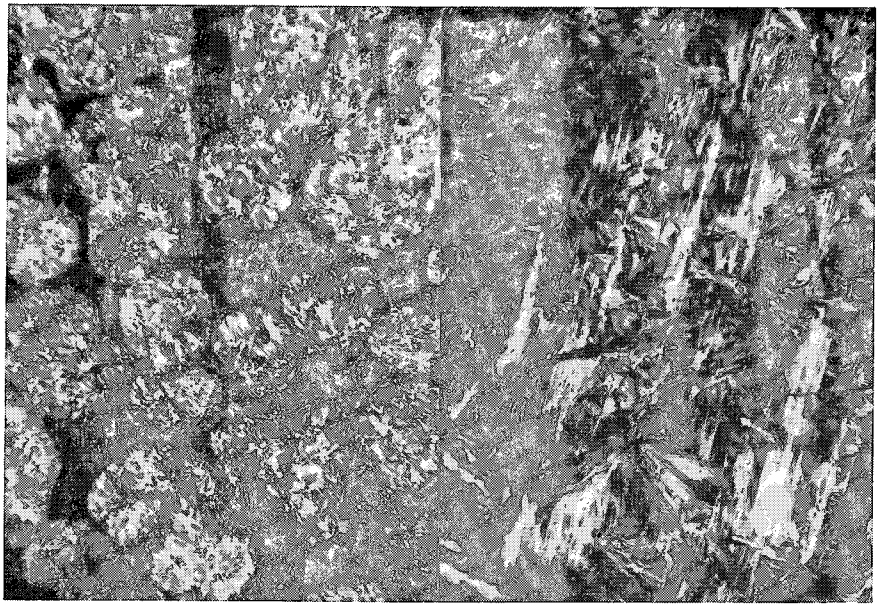

FIG. 7. Antigorite, pseudomorphic after olivine and pyroxene in a poikilitic texture. Parallel lines of fine granular magnetite identify original pyroxene cleavage. #82—Ospwagan Lake. (×25).

FIG. 8. Fibrolamellar, feathery flakes of antigorite in antigorite serpentinite. Preferred orientation indicates probable pyroxene pseudomorph. #82—Ospwagan Lake. (×62).

made by x-ray diffraction pattern, following the method of Whittaker & Zussman (1956), and by differential thermal analysis.

Although antigorite is not common in the nickel belt serpentinites, it is the principal serpentine mineral in a number of other serpentinized ultramafic rocks in Manitoba. Three samples from widely scattered localities were selected for comparison with the nickel belt antigorite and fibrous serpentines. A specimen of serpentinite from Knee Lake (Fig. 1, #305) contains a mixture of fine grained platy antigorite interspersed with areas of apparent fibrous material. The latter is not cross-fibre vein serpentine as described above, but appears rather as a series of short plates arranged side by side in a row and joined by a colourless fine grained isotropic strip to an adjacent row. When these are close packed, they have the appearance of interfering cross-fibre veinlets and may also form "hour-glass" textures (Fig. 9). The direction of apparent fibrosity has positive elongation as does the finer grained material in the rock. Although the texture shown in Fig. 9 has the form and optical elongation of gamma serpentine typical of mesh textures, there is no

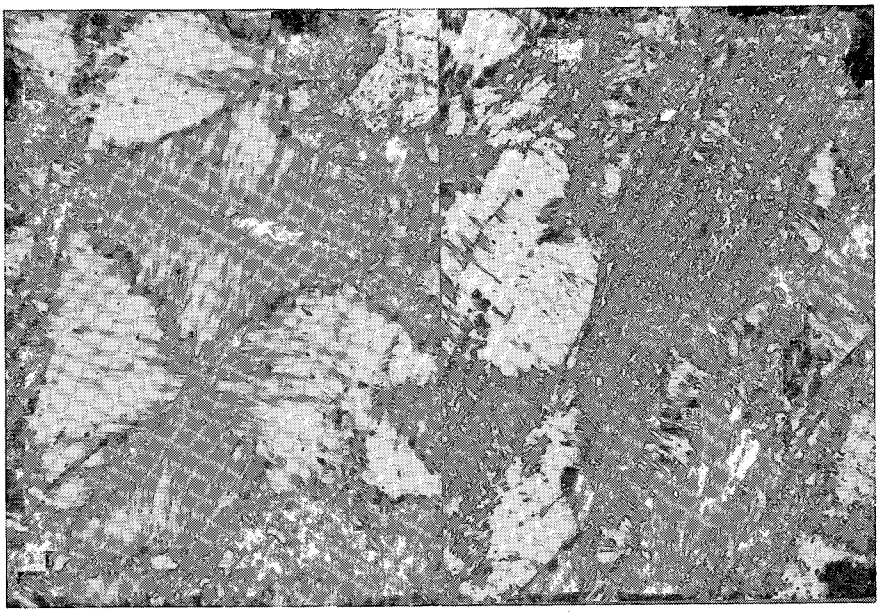

FIG. 9. "Hour-glass" texture in antigorite. Fibrolamellar plates arranged in the manner common to gamma serpentine. Magnetite is present in median (right centre) but not in black cross. #305—Knee Lake. (×169).

FIG. 10. Broad fibrolamellar plates of antigorite surrounded by fine grained platy antigorite. The latter shows preferred orientation in some areas. #310—Carrot River. (×31).

equivalent rim material with opposite elongation. Identification by x-ray diffraction pattern has shown this material to be entirely antigorite.

Fig. 10 illustrates the texture of an antigorite serpentinite from the Carrot River (Fig. 1, #310). The rock is similar to the Knee Lake serpentinite in showing a highly variable grain size and in the arrangement of elongated antigorite flakes to form short vein-like sections of aggregates. Elongation is positive.

A third and somewhat unusual serpentinite is found east of Linklater Island in Island Lake (Fig. 1, #311). Talc and carbonate form the matrix to pale green, faintly pleochroic, remnant pieces of serpentine. These fragments vary greatly in size and shape. Their most interesting feature is the nature of their fibrous structure. In equidimensional plates, a knife-edge seam, equal in length to about one quarter the width of the plate, is present at the centre. From this seam, fibres radiate out in all directions in a gentle s-shaped pattern. Extinction sweeps around the plate as a vague cross. In elongated fragments the central seam is longer and the pattern approaches that of bipartite cross-fibre veinlets. Thin concentric

banding is occasionally present towards the outer margin of the plates, and these show a slightly higher birefringence. The fibrous material has negative elongation. Minute opaque grains of probable magnetite are disseminated throughout. Commonly the radial fibrous plates are separated or partially encircled by narrow cross-fibre veinlets also having negative elongation and which are usually clouded with aggregates of magnetite. Talc and carbonate appear to have replaced the greater proportion of these in preference to the radial plates. It seems that the fibrous plates and marginal veins formed a mesh texture composed entirely of alpha serpentine.

Excellent evidence of the replacement of fibrous serpentine by antigorite is shown by a specimen from Island Lake, close to that described above (Fig. 1, #312). Alteration is restricted to spotted anhedral masses of carbonate. Approximately 20–30% of the rock is antigorite occurring as groups of pointed laths and spear-shaped crystals cutting through mesh serpentine and the carbonate aggregates which replace it (Fig. 11). Antigorite also cuts through narrow veinlets of cross-fibre chrysotile asbestos, which transect the serpentinite. Magnetite is abundant throughout the mesh serpentine and carbonate but is deficient in areas of new antigorite growth. Optically the antigorite is negative, $2V = 35°–45°$ (estimated), has positive elongation and straight extinction. The DTA curve of this rock confirms the presence of the two serpentine minerals.

Returning to the serpentinites of the nickel belt, it can be stated with reasonable certainty that massive antigorite serpentinites are exceedingly rare. The Ospwagan Lake occurrence (#82) is the only one identified as such at the present time. Late antigorite flakes replacing mesh serpentine have been identified in serpentinite from Setting Lake (#5) and in a serpentinite body located midway between Thompson and Ospwagan Lake (#160). In both specimens however, the minor quantity of antigorite present negated the possibility of its being identified by x-ray diffraction or DTA.

The origin and mode of occurrence of antigorite has been widely discussed in the literature, with a general agreement that it usually replaces mesh serpentine. Its formation has been ascribed to conditions of high pressure (Benson 1926), and to shearing stress accompanying metamorphism above the chlorite-biotite subfacies of the greenschist facies but equal to or slightly less than the albite-epidote amphibolite facies (Hess, Smith & Dengo 1952). Origin of antigorite by pure thermal metamorphism is considered probable by Wilkinson (1953) and Durrell (1940). The Ospwagan Lake antigorite shows relict textures of a primary peridotite (Fig. 7), in no way deformed or altered by shearing. On the other hand, a body of intrusive granite occurs at the north end of the lake,

FIG. 11. Antigorite flakes spearing and replacing fibrous serpentine (grey) and carbonate (dark grey). #312—Island Lake. (×70).

FIG. 12. Fine grained lizardite between cross-fibre veinlets of clinochrysotile. #122—Pipe mine. (×135).

within one-half mile of the sample location (Zurbrigg 1963). It is of interest that specimens from the west side of the Ospwagan ultramafic body are composed entirely of fibrous serpentine with no evidence of antigorite. Thus, if the antigorite serpentinite has developed from an original fibrous mesh-texture serpentinite, there now exists no remnant fibrous serpentine although there is preserved the original texture of the primary peridotite. Thermal metamorphism is considered the most likely cause for this development.

Lizardite

Two serpentine polymorphs are recognizable optically and by x-ray diffraction pattern in a specimen selected from the dump at the Pipe mine exploration shaft. (Fig. 1, #122). Subparallel cross-fibre veinlets of clinochrysotile are separated by narrow lensoid areas of fine grained lizardite (Fig. 12). The latter form a felt-like dense mass of inter-woven fibrolamellar platelets which constitute about 20% of the rock. Elongation of the plates appears to be positive. The chrysotile veinlets are 0.3 mm in width and have highly serrated margins. Each veinlet has a clear and colourless central spine which may contain oriented magnetite grains.

Elongation of the fibres is positive, which makes them optically comparable to fibres of gamma serpentine.

Review of Serpentine Structures

The classification of the serpentine minerals was considerably clarified by the work of Whittaker & Zussman (1956). They not only listed the distinctive *x*-ray diffraction characteristics of the two known serpentine varieties, chrysotile and antigorite, but they also recognized the existence of a third variety which they called lizardite. The serpentine group of minerals was thus found to be composed of three types or sub-groups. Although each of the three sub-groups have the same layered silicate structure, the Mg analogue of kaolinite, they each have their own distinctive structural variations. In chrysotile the layers are curved to form a cylindrical structure and a two layer unit cell must be used to index all reflections (Whittaker, 1953, 1956a, 1956b, and 1956c). In antigorite the layers are slightly curved in a definite manner so that a super period is produced along the *a* axis. (Aruja 1945; Zussman 1954; Kunze 1956 and 1958, Zussman, Brindley & Comer 1957). A single layer unit cell with a large *a* dimension must be used to index all reflections. Lizardite is composed of flat ortho-hexagonal layers stacked over each other with varying degrees of three-dimensional order. The diffraction data can be indexed using a single layer unit cell, but this simple model does not fit the observed diffraction data exactly (Whittaker & Zussman 1956) and a later work by Rucklidge & Zussman (1965) has shown that a complex model using both one layer and two layer units gives the best fit with the observed reflections.

Recognition of the existence of the flat ortho-hexagonal type of structure, and the production of certain synthetic serpentines (Roy & Roy 1954) lead to further discoveries. Zussman & Brindley (1957) showed that a serpentine mineral forming veins in chromite-bearing serpentine rock, originally described by Brindley & von Knorring (1954) as an ortho-hexagonal antigorite with a probable superlattice parameter along the *a* axis, actually had a 6-layer ortho-hexagonal cell with the large parameter along the *c* axis. Gillery (1959) produced various types of synthetic aluminous serpentines. Some were made up of a single ortho-hexagonal layer and gave diffraction patterns identical to lizardite, but two other types, with 6-layer ortho-hexagonal structures, were also found. One approximately a 3-layer structure, the other a 2-layer structure and Gillery called them 6 (3)-layer and 6 (2)-layer serpentines respectively. Naturally occurring aluminous serpentines with the 6 (3) and 6 (2)-layer structures were found as accessory minerals in iron ores from the Tracy

mine, Michigan (Gillery 1959; Bailey & Tyler 1960). Following this, Olsen (1961) reported a 6 (2)-layer orthohexagonal serpentine occurring in veins cutting a serpentinite sill at Thompson Lake, Labrador. Müller (1963) found a 6-layer serpentine forming veins and partially replacing the wall rock serpentine in a serpentinite at Maloja, Switzerland. Jahanbagloo & Zoltai (1966) have reported a 9-layer hexagonal aluminous serpentine occurring in vugs in a Lake Superior, Minnesota beach pebble of Keweenawan rhyolite. This sample possessed a 3-layer sub-cell building up to a 9-layer structure.

In these prior descriptions of ortho-hexagonal serpentines, the materials studied have been either vein-forming serpentines that cut serpentinites, accessory minerals in other rocks, or synthetic serpentine minerals. The present study is entirely directed toward the rock-forming serpentine minerals that make up the bulk of certain serpentinite intrusive bodies.

X-RAY DIFFRACTION DATA

The *x*-ray powder diffraction patterns of most of the fibrous serpentines from the nickel belt resemble in some ways the pattern from 6-layered serpentine as recorded by Zussman & Brindley (1957). However the consistent absence of the high intensity reflections 209(d = 2.335 Å), 2.0.15(d = 1.963 Å) and 2.0.21(d = 1.636 Å) and a number of weaker reflections, indicated that the mineral could not be correlated with any previously recorded form. Comparison of the spacings with those of the 6-layer type revealed that the principal difference lay in the almost total absence of *hkl*'s with *l* odd. This suggested that the pattern could be indexed on the basis of a 3-layer cell.

Using selected reflections from the diffraction pattern of specimen #88 from the Pipe mine (Fig. 1), together with the appropriate indices from the 6-layer type of Zussman & Brindley (1957) and assuming orthorhombic symmetry, the cell dimensions used for indexing were derived as follows:

00*l*	d(00*l*) Å	d(001) Å	
006	7.37	44.22	
0.0.12	3.66	43.92	Average d(001) = 43.86 Å
0.0.24	1.824	43.78	For new 3-layer cell c = 21.930 Å
0.0.30	1.463	43.89	
0*k*0	d(0*k*0) Å	d(010) Å	
020	4.60	9.20	Average d(010) = 9.205 Å
060	1.535	9.21	b = 9.205 Å
*h*0*l*	d(*h*0*l*) Å		
206	2.498		a = 5.346 Å

The best c parameter for the new 3-layer structure is 21.930 Å, which is slightly greater than half the value (43.59 Å) used by Zussman & Brindley. Indexing of all reflections was done by IBM 1620 computer using a Fortran program written for the purpose. The program calculates the d values for all possible hkl's which lie within narrow limits of variation from the d(obs.) spacings. The limits of variation are as follows: for $d > 3.0$ Å, ± 0.15 Å, for $d = 2.0 - 3.0$ Å, $\pm .0.05$ Å and for $d < 2.0$ Å, ± 0.02 Å.

Indexing was carried out on the combined reflections obtained from 15 specimens of pure serpentinite from scattered locations along the nickel belt whose diffraction patterns indicated essentially identical structures. Diffraction patterns from 4 of these samples (nos. 5, 88, 155, 189, Fig. 1) are reproduced in Fig. 13. Diffraction patterns of an additional 10 nickel belt serpentinites were similar, but contained extra peaks which could be attributed to the presence of such minerals as tremolite, chlorite and dolomite. The latter are not included in the present work. The results obtained are condensed and presented in Table 1, using the recorded data on the 6-layer ortho-type for comparison. The d(obs.) values listed are for the predominant reflections from the 15 pure specimens. Slight variations from these values in what are considered to be equivalent spacings, are probably due to minor differences in the serpentine compositions, combined with the errors involved in measuring the maxima of poorly defined peaks. Where more than one hkl is listed for a particular d(calc.) value the first one corresponds to that value and the additional ones, either to that value also or to d(calc.) values extremely close to values of d(obs.).

Prominent differences between the 6-layer ortho-type of Zussman & Brindley (1957) and the 3-layer ortho-type in the Manitoba serpentinites are readily observable from Table 1. With certain exceptions the hkl's with l odd in the 6-layer cell are missing in the 3-layer type. Exceptions to this are the 203 reflection ($d = 2.623$ Å), which may not be strictly equivalent to the 2.652 Å reflection of the 3-layer type, the 0.2.15 reflection ($d = 2.450$ Å) and the 409 reflection ($d = 1.283$ Å). The low intensity 0.2.10 reflection ($d = 3.17$ Å) of the 6-layer cell has no recognizable equivalent in the 3-layer pattern. Diffractogram records were not obtained beyond the angle $2\theta = 75°$ so that the smallest spacing recorded for the 3-layer type is 1.281 Å. It can be seen that the derived 3-layer orthorhombic cell with $a = 5.346$ Å, $b = 9.205$ Å, $c = 21.93$ Å (3×7.31 Å), gives good agreement between observed and calculated d values for a wide range of reflections.

As previously mentioned, the only known occurrence of antigorite serpentine along the nickel belt is found at Ospwagan Lake. The x-ray

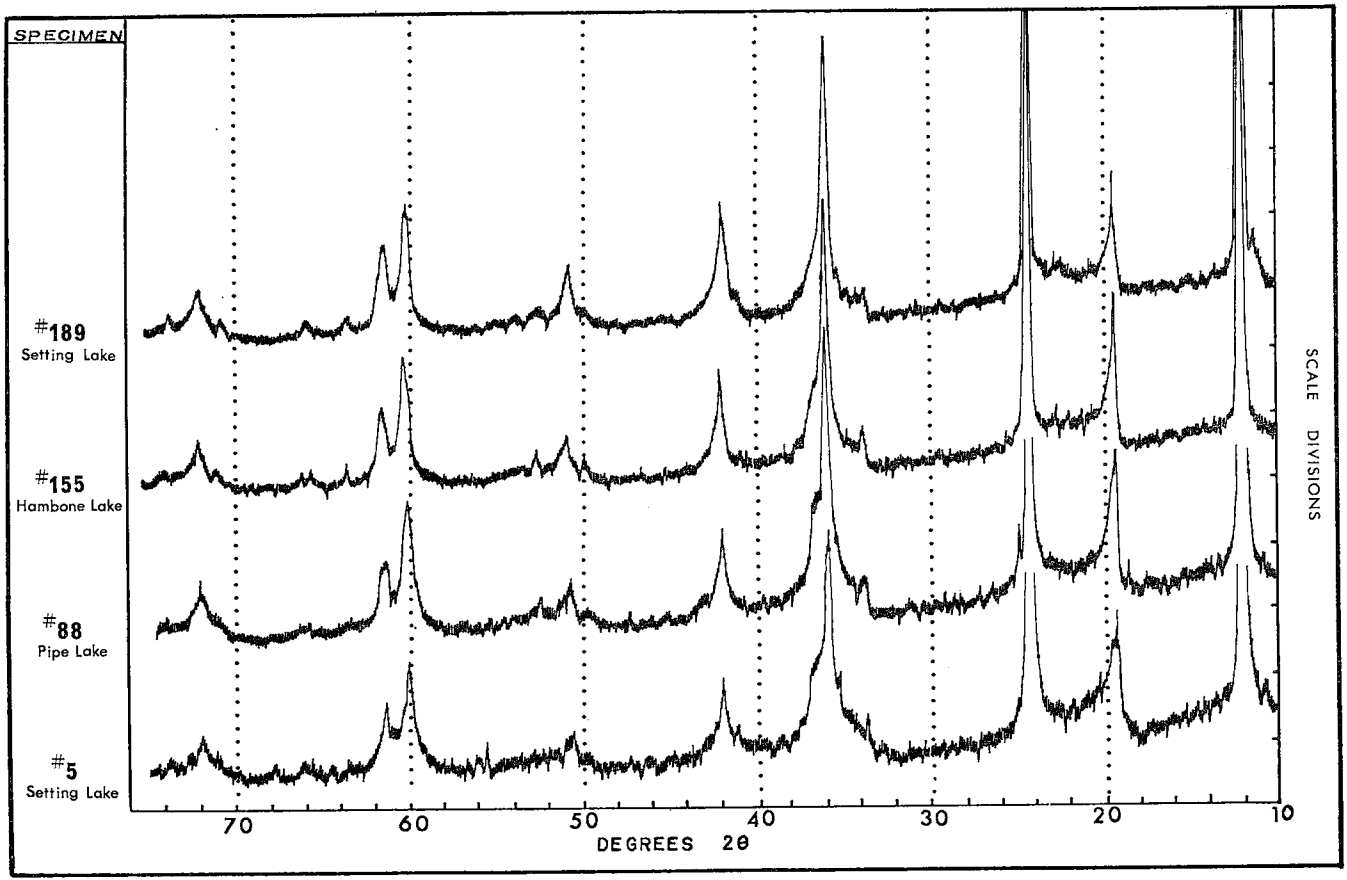

FIG. 13. *X*-ray powder diffraction patterns of 3-layer serpentines from the Manitoba nickel belt. CuK_α radiation.

TABLE 1. COMPARISON OF X-RAY POWDER DIFFRACTION DATA OF 6-LAYER AND 3-LAYER SERPENTINES

6-layer Ortho-type*			3-layer Ortho-type†			
d	*I*	*hkl*	*d* (obs)	*Ic/s*	*d* (calc)	*hkl*
7.33Å	100	006	7.40Å	400	7.310Å	003
4.60	60	020	4.60	76	4.602	020
4.40	10	023				
4.25	10	024	4.28	20	4.243	022,112
4.09	10	025				
3.90	5	026	3.90	36	3.894	023,113
3.66	100	0.0.12	3.66	225	3.655	006
3.53	5	028	3.52	16	3.525	024,114
3.35	5	029				
3.17	5	0.2.10				
3.02	5	0.2.11				
2.865	5	0.2.12	2.867	9	2.867	026,116
2.720	5	0.2.13				
2.623	30	203	2.652	20	2.653	201,018
2.502	100	206	2.502	141	2.500	133,212
2.450	10	0.2.15	2.442	47	2.439	108
2.335	70	209				
2.149	60	2.0.12	2.151	45	2.151	136
1.963	70	2.0.15				
1.815	5	0.0.24	1.824	12	1.827	0.0.12,052
1.791	10	2.0.18	1.791	26	1.792	0.1.12,139
1.739	10	310	1.740	16	1.740	150,241
1.636	40	2.0.21				
1.535	80	060	1.537	73	1.537	331,060
1.501	70	2.0.24	1.505	46	1.506	1.3.12,0.4.11
1.452	2	0.0.30	1.463	10	1.461	0.0.15,254,162
1.415	20	0.6.12	1.415	9	1.416	159,066
1.379	20	2.0.27				
1.327	10	403				
1.309	50	406	1.309	28	1.309	263
1.296	2	0.6.18				
1.283	5	409	1.281	12	1.281	421,1.3.15
1.276	5	2.0.30				
1.210	10	0.0.36				
1.182	2	2.0.33				
1.168	5	4.0.18				
1.121	5	4.0.21				

*Data from ASTM 9–444 (Rf. Zussman & Brindley 1957).

†*d*(obs) are significant reflections from 15 pure samples (5, 39, 88, 91, 96, 107, 110, 128, 140, 155, 157, 160, 189, 190, 206). *I* c/s-Intensity measured as counts/seconds on $4x10^2$ scale. *d*(calc) and *hkl* derived from assumed cell dimensions of $a = 5.346$Å $b = 9.205$Å $c = 21.930$Å. For diffractometer operating data, see text.

diffraction pattern of a specimen from this occurrence (#82) is reproduced in Fig. 14, along with patterns from the Carrot River, Manitoba (#310) and from specimen 481–7 (Museum No.—Dept. of Geology) labelled "williamsite", Lancaster Co. Pa. Details of the diffraction patterns are listed in Table 2, together with the data from the Caracas antigorite described by Hess, Smith & Dengo (1952) and listed in the ASTM file, card 7–417. Specimen 481–7 (williamsite) from the Mineral Museum of

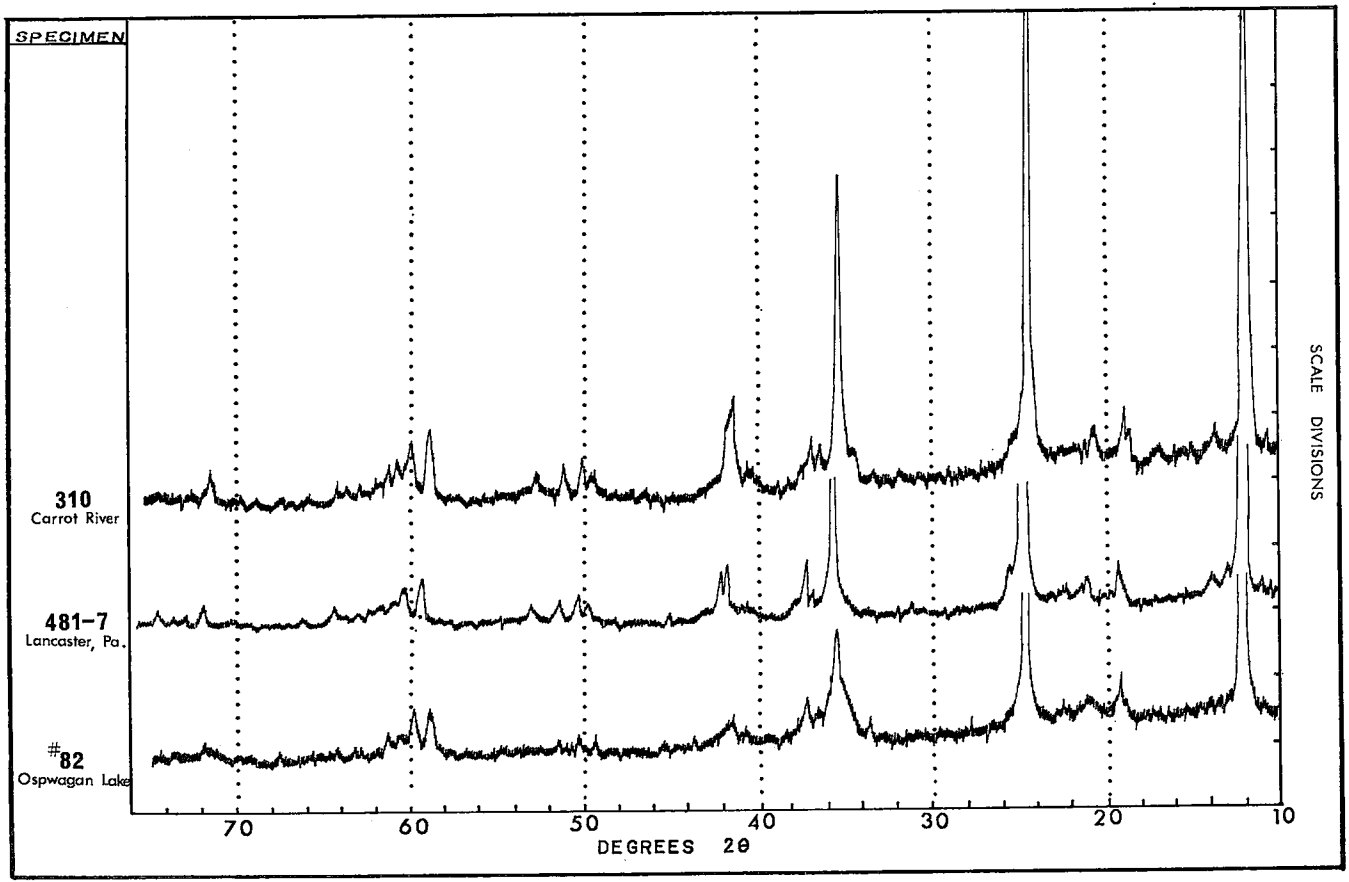

FIG. 14. *X*-ray powder diffraction patterns of antigorite. CuK_α radiation.

TABLE 2. *X*-RAY POWDER DIFFRACTION DATA OF ANTIGORITES*

ASTM. 7–417			82		481–7		310	
d	*I*	*hkl*	*d*	*I*	*d*	*I*	*d*	*I*
8.05Å	10				7.9Å	25	8.14Å	18
7.30	400	001	7.31Å	400	7.20	1000	7.31	400
6.95	24	$20\bar{1}$			6.78	48	6.84	17
6.51	16	$30\bar{1}$			6.32	36	6.39	22
6.10	6	–						
5.78	8	401			5.72	13	5.83	9
							5.18	7
4.67	6	810					4.66	33
4.62	7	020	4.62	26	4.57	62		
4.27	4	$9\underline{10}$	4.21	12	4.19	42	4.27	20
4.01	6	$8\bar{1}\bar{1}$	3.95	10	3.97	35		
3.63	300	102	3.63	256	3.59	1000	3.64	400
3.51	24	$30\underline{2}$	3.51	11	3.48	70	3.51	18
2.88	2	$14.0.\bar{1}$			2.87	28		
			2.66	12				
2.59	4	930						
2.57	8	17.0.0			2.57	32	2.59	22
2.52	70	$16.0.\underline{1}$	2.53	76	2.51	320	2.53	188
2.46	9	$93\bar{1}$	2.46	22	2.44	40	2.46	28
2.42	38	003	2.42	28	2.41	85	2.42	32
2.39	9	17.0.1	2.38	17	2.37	35	2.39	14
2.35	5	403					2.35	6
2.237	6	$15.0\underline{2}$			2.238	20	2.238	11
2.208	7	$16.0.\bar{2}$	2.21	11	2.201	20	2.222	18
2.167	22	$83\bar{2}$	2.161	20	2.161	80	2.176	58
2.150	20	$16.0.\underline{2}$	2.141	11	2.144	78	2.166	48
2.126	4	$93\underline{2}$						
					2.10	20		
2.035	4	$11.3.\bar{\underline{2}}$			2.011	13		
1.886	3	$15.0.\bar{3}$						
1.830	12	15.0.3	1.845	10	1.831	28	1.838	18
1.815	23	$00\underline{4}$	1.811	12	1.810	45	1.817	24
1.781	14	$93\bar{3}$			1.778	35	1.779	22
1.755	4	$10.3.\bar{3}$						
1.736	10	17.0.3			1.728	28	1.738	16
1.688	2	$21.3.\underline{1}$						
1.640	2	21.3.1						
1.640	2	$22.3.\underline{1}$						
1.584	3	$17.0.\bar{4}$						
1.560	12	24.3.0	1.565	28	1.556	75	1.569	44
1.540	9	$06\underline{0}$	1.542	32	1.537	60	1.542	36
1.535	9	$24.3.\underline{1}$			1.532	60	1.533	26
1.524	13	15.0.4	1.528	14	1.521	40	1.523	22
1.509	8	$06\underline{1}$	1.509	12	1.503	30	1.512	21
1.497	10	$17.0.\bar{4}$	1.497	6	1.493	26	1.496	15
1.479	7	$93\underline{4}$	1.471	8	1.475	17	1.477	8
1.466	6	$18.0.\bar{4}$						
1.462	6	$10.3.\underline{4}$						
1.451	10	$20\bar{5}$	1.453	6	1.459	21	1.461	10
1.448	9	205			1.446	32	1.449	12
1.443	5	–						
1.438	3	–					1.419	6
1.328	3	–					1.326	23
			1.313	10	1.313	32		
					1.297	16		
					1.275	24		

*Specimens: ASTM 7–417 (Ref. Hess, Smith & Dengo 1952), Caracas, Venezuela. 82 — Ospwagan Lake, Man. 481–7 — Lancaster Co., Pa. 310 — Carrot River, Man. For diffractometer operating data, see text.

the Department of Geology, University of Manitoba, is a bluish green, translucent, massive serpentine with a spintery fracture. A similar specimen has been investigated by Faust & Fahey (1962, #F–1, p. 8) and classified by them as antigorite. The nickel belt antigorite in hand specimen is dark greyish-green and massive, and the Carrot River sample, dark green, fine grained and massive. Thus although these three specimens differ considerably in physical appearance, their *x*-ray diffraction patterns (Fig. 14) indicate they possess identical structures.

Differential Thermal Analyses

Some typical and representative DTA curves for the 3-layer serpentine are shown in Fig. 15. The major thermal effect evident in these curves begins at approximately 600° C, where the loss of constitutional water initiates the breakdown of the structure. The resultant endothermic trough reaches a minimum at a temperature between 660°–675° for the samples examined. The trough is thus a record of the heat absorption accompanying the destruction of the serpentine, a process which is normally complete by 700° C. A prominent exothermic peak occurs between 803–815° C, and is related to the formation of forsterite. The height or intensity of this peak is very variable (Figs. 15E and 15F), and it does not appear to be related to the intensity or temperature of the endothermic trough. It possibly bears a relationship to the composition of the olivine generated, but this remains to be determined. Faust & Fahey (1962) found no simple relationship of area and height of peak to the amount of sample used in the heating experiments. Small irregularities in the pattern of curves 15B and 15E are likely due to the presence of minor quantities of contaminating minerals.

DTA curves for specimens of antigorite are shown in Fig. 16. Two curves, 16A and 16B, for sample #82 from Ospwagan Lake are compared with those for three additional antigorite specimens from Manitoba, and to the specimen of "williamsite" (curve 16F), described above. The decomposition of antigorite takes place on heating in the 700–800° C range. Antigorite can thus be easily distinguished by DTA from the fibrous serpentine minerals. In the samples examined, the minima of the endothermic trough varied between 750–775° C. For specimen #82 a minimum at 750° C was obtained when heated in a nitrogen atmosphere compared with a temperature of 775° C when heated in air. Apart from 16B, the curves were all obtained without the use of an artificial atmosphere. Immediately following the major endotherm a small exotherm is usually present between 810–815° C, presumably related to the crystallization of olivine as a new phase. A small bow-shaped endotherm is

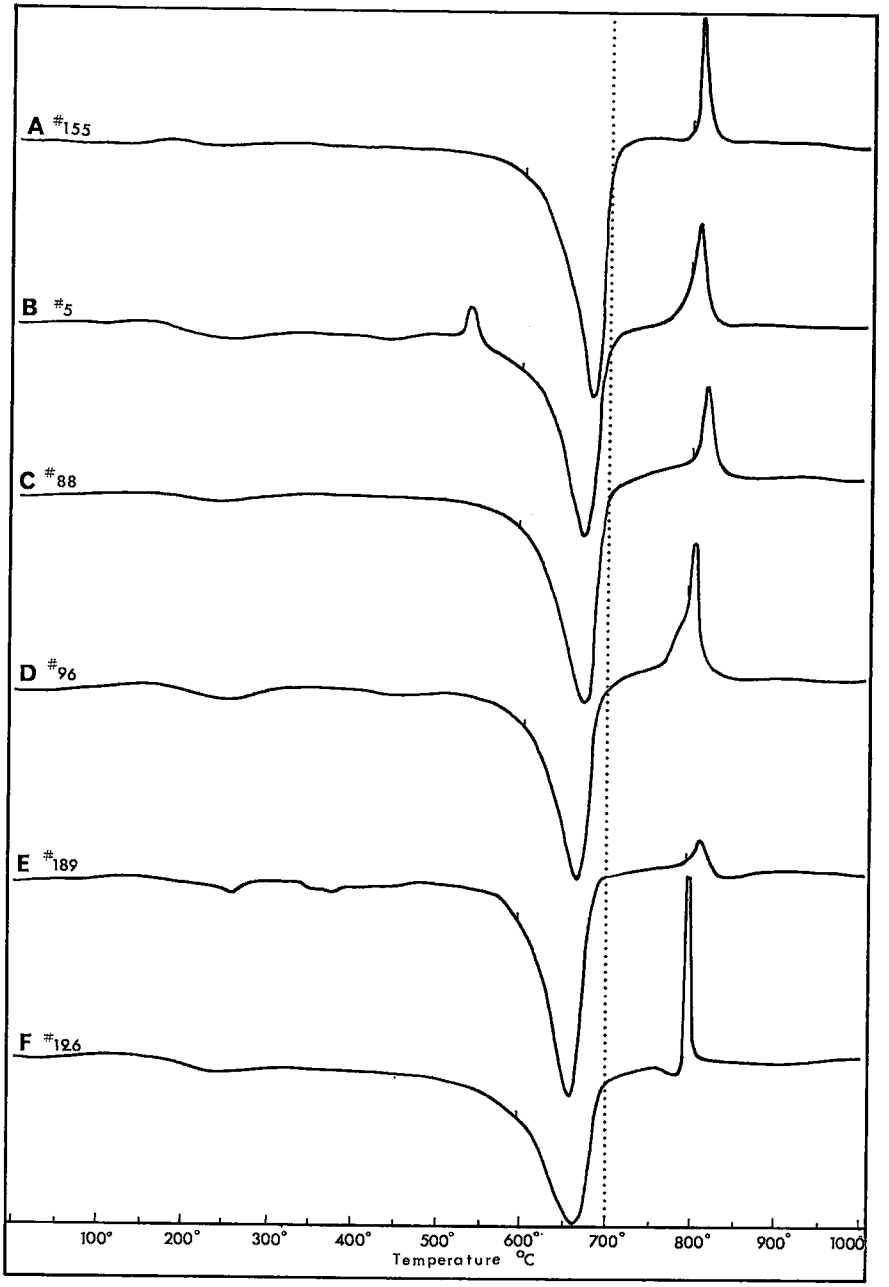

FIG. 15. DTA curves of 3-layer serpentines from the nickel belt.

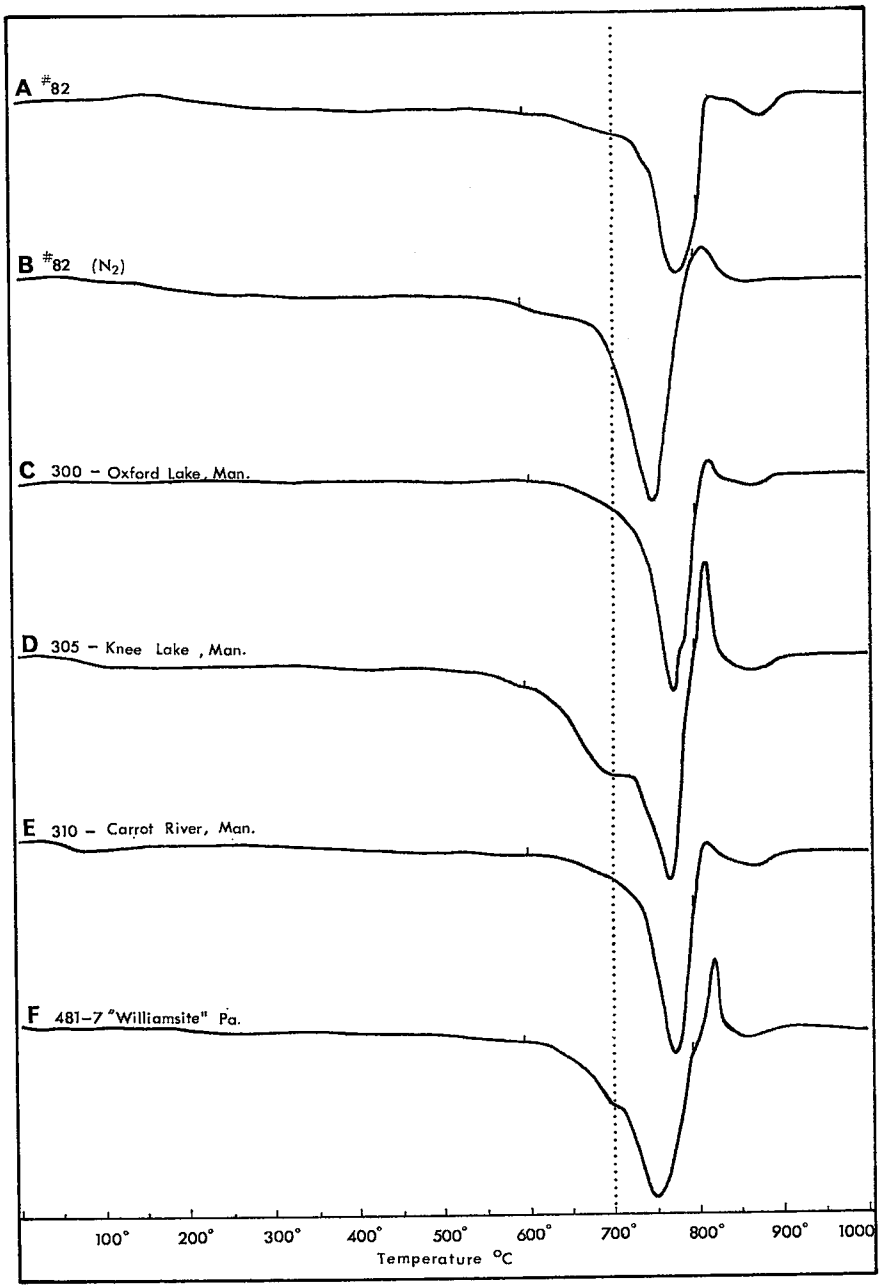

FIG. 16. DTA curves of selected antigorites.

generally present in the 850–875° C range. This has been attributed to a possible phase transformation (Faust & Fahey 1962). A slight inflection on the low temperature side of the major endothermic trough has been noted by a number of writers, and is a prominent feature of curves 16D and 16F. Faust & Fahey attribute the inflection to 1) the presence of chrysotile in the sample, 2) heterogeneity within the sample itself or 3) nonequilibrium factors. It is interesting to note that curve C-124 (p. 73) of those writers is not directly comparable to curve 16F above, and yet both are specimens of pure antigorite ("williamsite") from the same locality. Factors 2 and 3 therefore, may be important in producing certain features in DTA curves.

Below 600° and above 900° C, the antigorite curves are essentially straight lines. The complete absence or the very reduced size of the exothermic peak in antigorites as compared to that in chrysotiles and other fibrous serpentine minerals has been discussed by Caillère & Hénin (1957). This feature depends on the temperature interval between dehydroxylation and recrystallization. In the chrysotiles, the interval is large, represented on the thermal curves by a nearly straight line. Sample material examined from this range is amorphous. Specimens of antigorite which have next to no exothermic peak, have been found to contain forsterite at a temperature slightly before the end of the endothermic peak.

Summary and Conclusions

The optical investigation of Manitoba's nickel belt serpentinites shows them to be composed of fibrous material with two optical orientations, alpha serpentine and gamma serpentine. The predominant fibre type is alpha serpentine with negative elongation. Fibrous material has three textural arrangements: (1) mesh texture serpentine with a more or less regular disposition of mutually interfering cross-fibre veinlets; (2) close-packed parallel veinlets and (3) a highly irregular branching network of veinlets with variable interstitial material. Pseudomorph boundaries in all three types are generally discernible. Antigorite of later replacement origin has been identified in a small number of serpentinites. One known occurrence at Ospwagan Lake is entirely composed of antigorite and is believed to have originated by the thermal metamorphism of fibrous serpentine. From a variety of textural features, the original rocks are considered to have been dunites and olivine-rich peridotites.

More detailed examination of the fibrous serpentine composing the majority of the nickel belt serpentinites, by x-ray diffraction procedures on powdered samples, has shown it to be a type which is not directly comparable to chrysotile. X-ray powder patterns of this serpentine can

be satisfactorily indexed on the basis of a 3-layer orthorhombic cell with dimensions of $a = 5.346$ Å, $b = 9.205$ Å, $c = 21.930$ Å. The c parameter is approximately one half the value of that used by Zussman & Brindley (1957) in indexing a 6-layer serpentine from Unst. *X*-ray diffraction studies have also indicated a mixture of clinochrysotile and lizardite in a specimen from the stockpile near the exploration shaft of the Pipe mine, and verified the occurrence of antigorite at Ospwagan Lake. Comparison has been made, by the diffraction powder patterns, of these minerals with antigorite serpentinites from Carrot River in Manitoba and with the well-known occurrence of antigorite ("williamsite") from Lancaster Co., Pennsylvania.

Differential thermal analyses of the nickel belt serpentinites show that the heating curves derived from the fibrous 3-layer serpentines are essentially identical to those obtained from chrysotile (Faust & Fahey 1962). For identification between them, reliance must be made on *x*-ray diffraction methods. DTA curves of antigorite are readily identified.

Acknowledgments

The writer wishes to thank Professor R. B. Ferguson of the Department of Geology, University of Manitoba for his assistance during the period of research on this project and for critically reading the manuscript. Sample material was supplied by Falconbridge Nickel Mines Ltd., and International Nickel Company with the permission of Mr. G. P. Mitchell and Mr. J. Keith Diebel, which is greatly appreciated. Thanks are also due to Dr. A. R. Graham and Dr. J. J. Brummer of Falconbridge and to Mr. F. J. Wicks for helpful discussions and material assistance, and to Mr. R. Pryhitko for the photography. Permission to publish this paper was received from Falconbridge Nickel Mines Ltd. and the International Nickel Co. of Canada Ltd.

References

Aruja, E. (1945): An x-ray study of the crystal structure of antigorite, *Min. Mag.*, **27**, 65–74.

Bailey, S. W., & Tyler, S. A. (1960): Clay minerals associated with the Lake Superior iron ores, *Econ. Geol.*, **55**, 150–175.

Barry, G. S. (1959): Geology of the Oxford House-Knee Lake area, *Man. Mines Br. Publ.* **58–3**.

——— (1960): Geology of the Western Oxford Lake-Carghill Island area, *Man Mines Br. Publ.* **59–2**.

Benson, W. N. (1926): The tectonic conditions accompanying the intrusion of basic and ultrabasic igneous rocks, *Mem. Nat. Acad. Sci.*, **19**, no. 1, 1–90. Washington.

Brindley, G. W., & von Knorring, D. (1954): A new variety of antigorite (orthoantigorite) from Unst, Shetland Islands, *Amer. Min.*, **39**, 794–804.

CAILLÈRE, S., & HENIN, S. (1957): The chlorite and serpentine minerals: in *The Differential Thermal Investigation of Clays*. R. C. Mackenzie, ed., Min. Soc. London. Ch. V111.

COATS, C. J. A. (1966): Serpentinized ultramafic rocks of the Manitoba nickel belt, *Unpub. Ph.D. thesis, Univ. of Manitoba, Winnipeg.*

DEER, W. A., HOWIE, R. A., & ZUSSMAN, J. (1962): *Rock-Forming Minerals*, vol. 3, Sheet Silicates, 1–270.

DURRELL, C. (1940): Metamorphism in the Southern Sierra Navada, northeast of Visalia, California, *Univ. of California, Dept. of Geol. Sci., Bull.*, **25**(1), 1–117.

FAUST, G. T., & FAHEY, J. J. (1962): The serpentine-group minerals, *USGS. Prof. paper* **384-A**, 1–87.

FRANCIS, G. H. (1956): The serpentinite mass in Glen Urquhart, Inverness-shire, Scotland, *Am. Jour. Sci.*, **254**, 201–226.

GILLERY, F. H. (1959): The x-ray study of synthetic Mg-Al serpentines and chlorites, *Amer. Min.*, **44**, 143–152.

GODARD, J. D. (1963): Geology of the Island Lake-York Lake area, *Manitoba Mines Br. Publ.* **59–3**, 1–45.

HESS, H. H., SMITH, R. J., & DENGO, G. (1952): Antigorite from the vicinity of Caracas, Venezuela, *Amer. Min.*, **37**, 68–75.

JAHANBAGLOO, I. C., & ZOLTAI, T. (1966): The crystal structure of a hexagonal Al-serpentine, Abst. 5.54. 7th Inter. Cong. and Symp., International Union of Crystallography. *Supplement to Acta Cryst.*, **21**, A56.

KUNZE, G. (1956): Die Gewellte Struktur des Antigorits, I. *Zeit. Krist.*, **108**, 82–107.

——— (1958): Die Gewellte Struktur des Antigorits, II. *Zeit. Krist.*, **110**, 282–320.

MÜLLER, P. (1963): 6-layer serpentin vom Piz Lunghin Maloya, Schweiz. *N. Jb. Miner. Abh.*, **100**, 101–111.

OLSEN, E. J. (1961): Six-layer ortho-hexagonal serpentine from the Labrador Trough, *Amer. Min.*, **46**, 434–438.

PARRISH, W., and MACK, M. (1963): *Charts for the solution of Bragg's Equation. Data for X-ray analysis*, 2nd Ed., vol. 1. Philips Technical Library.

ROY, D. M., & ROY, R. (1954): An experimental study of the formation and properties of synthetic serpentines and related layer silicate minerals, *Amer. Min.*, **39**, 957–975.

RUCKLIDGE, J. C., & ZUSSMAN, J. (1965): The crystal structure of the serpentine mineral lizardite $Mg_3Si_2O_5(OH)_4$. *Acta Cryst.*, **19**, 381–389.

SELFRIDGE, G. C. (1936): An x-ray and optical examination of the serpentine minerals, *Amer. Min.*, **21**, 463–503.

WHITTAKER, E. J. W. (1953): The structure of chrysotile, *Acta. Cryst.*, **6**, 747–748.

——— (1956a): The structure of chrysotile II. Clinochrysotile, *Acta Cryst.*, **9**, 855–862.

——— (1956b): The structure of chrysotile III. Orthochrysotile, *Acta Cryst.*, **9**, 862–864.

——— (1956c): The structure of chrysotile IV. Parachrysotile, *Acta Cryst.*, **9**, 865–867.

——— and ZUSSMAN, J. (1956): The characterization of serpentine minerals by x-ray diffraction, *Mineral. Mag.*, **31**, 107–126.

WILKINSON, J. F. G. (1953): Some aspects of the alpine-type serpentinites of Queensland, *Geol. Mag.*, **90**, 305–321.

ZURBRIGG, H. F. (1963): Thompson Mine geology, *Trans. Can. Inst. Min. Met.*, **66**, 227–236.

ZUSSMAN, J. (1964): Investigation of the crystal structure of antigorite, *Min. Mag.*, **30**, 498–512.

——— and BRINDLEY, G. W. (1957): Serpentines with 6-layer ortho-hexagonal cells, *Amer. Min.*, **42**, 666–670.

——— BRINDLEY, G. W., and COMER, J. J. (1957): Electron diffraction studies of serpentine minerals, *Amer. Min.*, **42**, 133–153.

Manuscript received April 10, 1967, emended July 10, 1967